J Nanostruct 15(4): 1916-1924, Autumn 2025

RESEARCH PAPER

Fabrication of Electrospun PVA, PVC, and PU/PVC/WO_3 Nanofibers for X-ray Shielding

Homeyra Emad Abdoluosefi [1], *Ahmad Ramazani-Moghaddam-Arani* [1]*, *Ali Akbar Alizadeh* [2]

[1] *Department of Physics, University of Kashan, Kashan, Iran*

[2] *Department of Tissue Engineering & Applied Cell Sciences, Shiraz University of Medical Science, Shiraz, Iran*

ARTICLE INFO

Article History:
Received 19 May 2025
Accepted 23 September 2025
Published 01 October 2025

Keywords:
Electrospinning method
Half-value layer
Mechanical properties
PU/PVC/WO_3 nanofibers
X-ray shielding performance

ABSTRACT

WO_3 nanoparticles and polyurethane/polyvinyl chloride (PU/PVC) polymers were used to fabricate PU/PVC/WO_3 nanofibers mats with different percentages of WO_3 filler loading (0 – 35 wt. %) using an electrospinning method. Surface morphology and average diameter of composite nanofibers were determined by scanning electron microscope imaging. Fourier transforms Infrared spectra of the nanofibers were investigated, revealing displacement in the position of the bands and changes in their intensity depending on the filler loading. Also, a strength testing device is employed to study the mechanical properties of the nanofibers, indicating their high modulus of elasticity. The fabricated Pb-free electrospun nanofibers were exposed to an X-ray tube with voltages in the range from 20.3 up to 35 kV, and the effects of voltage, filler loading, and polymer type on the attenuation coefficient and half-value layer (HVL) are investigated. The HVLs of 35 and 30 wt. % WO_3 nanoparticle-filled PVC and PU/PVC nanofibers were 0.0156 and 0.0135 cm, being approximately 2.22- and 1.92-fold compared to those of Pb as evaluated by XCOM calculations at the low voltages. Therefore, the manufactured samples have a small half-value layer and at the same time, significantly low density as well as flexibility which can pave the way for their use in personal shielding in clinical and non-clinical applications. Due to the flexibility and low thickness of fabricated nanofibers, they can easily cover the irradiated organs and be good candidates for use as a light, lead-free, and efficient shield for X-rays in diagnostic imaging.

How to cite this article
Abdoluosefi H., Moghaddam-Arani A., Alizadeh A. Fabrication of Electrospun PVA, PVC, and PU/PVC/WO_3 Nanofibers for X-ray Shielding. J Nanostruct, 2025; 15(4):1916-1924. DOI: 10.22052/JNS.2025.04.038

INTRODUCTION

One of the most common methods utilized for diagnosis and treatment in medical fields is X-rays imaging [1], whereby about 80% of doses received by the patients are absorbed [2, 3]. Since the past few decades, lead has been one of the most effective materials for protection against gamma and X-ray radiation. However, due to its high toxicity, lead is harmful to humans and the environment. Moreover, the high weight of lead shielding makes it problematic to use it as a personal radiation protection material, especially for long-term uses [4, 5]. Therefore, researchers have been looking for methods to replace lead by materials with low density, low fabrication cost, and suitable mechanical properties, while also

* *Corresponding Author Email: ramezamo@kashanu.ac.ir*

being eco-friendly.

Based on these properties, nanofibers/ polymer composites have received special attention. According to recent studies, some nano composites such as lead (II) oxide, iron (III) oxide, copper (II) oxide, bismuth (III) oxide, gadolinium (III) oxide, and tungsten trioxide mixed with polyvinyl alcohol (PVA), epoxy resin, methyl vinyl silicone rubber, polyvinyl chloride (PVC), and polystyrene resin are considered suitable candidates for radiation shielding material [6, 7, 8, 9, 10, 11, 12, 13]. Among polymers, PVA has unique physical and chemical characteristics due to its hydrophilic and semi-crystalline nature. In addition, PVA polymer is inexpensive and has good chemical resistance, thermal stability, physical properties, and excellent biocompatibility [14].

On the other hand, polyurethane (PU) and PVC are the most widely used polymers in the world. The cheapest polymer available is PVC, having many advantages such as hardness and stiffness together with resistance to acids, alkalis, and corrosion [15, 16]. Nevertheless, owing to its resistance to wear and excellent plastic and elastic properties, PU has received more attention in a wide range of applications in the field of flexible and hard foam materials, water and air filters, optical filters, and protective clothing [17-19].

Theoretically speaking, since the attenuation coefficient is closely proportional to the fourth power of the atomic number (Z) of the absorber material, heavy elements can increase the mass attenuation coefficient and as a result the X-ray shielding performance, significantly. Notably, tungsten is a shielding material against X-rays, being proposed as a good alternative to Pb because of its high atomic number (Z = 74) and density (7.16 g cm−3) [2, 20, 21]. It is also possible to coat WO_3 compounds in polymer composite on fabrics as an effective approach to producing flexible, wearable, and lead-free aprons [22]. The electrospinning method has been suggested and employed successfully to fabricate nanofibers with an average diameter of a few nanometers to more than one micrometer. This method enables simple, large scale and cost-effective fabrication of nanofibers with unique features, including a high surface-to-volume ratio and excellent mechanical properties.

Also, the use of the electrospinning method can improve the dispersion of fillers (e.g., nanoparticles) in the polymer, thereby optimizing the properties of the resulting nanocomposites and reducing X-ray transmission [24, 25]. For example, using an electrospinning method, Jamil et al. have utilized WO_3 and Bi_2O_3 nanoparticles as the fillers of PVA polymer composites, providing high X-ray attenuation [2]. A study of the X-ray shielding performance of two different types of micro- and nano-sized WO_3 and Bi_2O_3 particles revealed that the filler size can affect the ability to attenuate X-rays [13, 24, 25, 26, 27, and 28]. However, there is no report on the fabrication, characterization, and shielding performance of electrospun PVC and PU/PVC nanofibers filled with WO_3 particles, according to the best of our knowledge

In this paper, X-ray protective nanofibers are fabricated by filling PU/PVC polymer with WO_3 nanoparticles as a filler material using an electrospinning method. The loading percentage of the filler is varied between 0-35wt%. Morphological, chemical, mechanical, and X-ray shielding properties of the resulting nanofibers are investigated. Moreover, PVA and PVC nanofibers filled with WO_3 nanoparticle composites are fabricated, and their performance is compared with that of PU/PVC/WO_3 nanofibers and also simulation calculations from XCOM [29] and reported data. This study evidences comparable performance of the electrospun nanofibers relative to Pb in terms of the attenuation coefficient, proposing them as highly efficient X-ray shielding materials.

MATERIALS AND METHODS

Commercial-grade polyurethane pellets (Apilon D1 70L, MW: 65000) were prepared from Applicazioni Plastiche Industriali Spa in Italy, and PVC was obtained from Bandar Imam Petrochemicals Co. in Iran. Also, tetrahydrofuran (THF) and N, N-dimethylformamide (DMF) (Samchun Pure Chemical Co., South Korea) were used as the solvents. PVA powder (molecular weight: 35,000 g mol^{-1}; density: 1.329 g cm^{-3}), WO_3 Nanopowder (particle size less than 100 nm; density: 7.16 g cm−3), used for synthesizing electrospun nanofibers were purchased from Sigma-Aldrich.

Electrospun nanofibers were fabricated by using an electrospinning machine (Asian Nanostructures Technology Company, Iran). The electrospinning technique consisted of various parameters such as the voltage, flow rate of solution through the

uniaxial needle, rotation speed of the collector (in rpm), and distance between the collector and the needle. To perform the electrospinning process, the mixed solutions were loaded into a 10 ml syringe pump with a 25-G needle. The electrospinning parameters were selected as follows:

- applied voltage = 20 kV,
- flow rate of solution = 1 ml hr−1,
- rotation speed of the collector = 500 rpm,
- and distance between the collector and the nozzle = 15 cm.

A very thin layer of oil was then rubbed on the surface of the aluminum foil so that the nanofibers could be easily removed from the foil surface without being damaged. To obtain an acceptable thickness for radiation attenuation tests, the nanofibers mats were collected on flat aluminum foil for 4 h. Two compounds of PVA/WO_3 and PU/PVC/WO_3 composite were fabricated with a concentration of 12% (W/V). Increasing the filler percentage is not stopped until the uniformity and mechanical properties decrease significantly. It should be noted that based on some studies beyond some point, the increment in mass attenuation coefficient becomes small even when the weight fraction of lead nanoparticles continues to increase [30].

X-ray attenuation measurement

A molybdenum X-ray tube with voltages ranging from 21 up to 35 kV and a current of 1 mA was used to provide a collimated X-ray radiation. The composite samples were exposed to the X-ray produced in each selected voltage. When a parallel beam of photons with the intensity of I_0 is irradiated on the composite sample with a thickness of x, the intensity of photons (I) emerging without having interacted with the target can be obtained from:

$$I = I_0 e^{-\mu x} \quad (1)$$

formula in which μ is the linear attenuation coefficient of sample and determined by measuring the intensity of the beam before and after passing through the sample. It should be noted that X-rays are collimated to a narrow beam before striking the absorber to establish good geometry conditions.

RESULTS AND DISCUSSION

Morphology of electrospun nanofibers

The morphology of nanofibers was investigated for three different polymers (PVA, PVC, and PU/PVC) filled with different loadings of WO_3 nanoparticles using SEM images, and the effect of the filler loading on the diameter of nanofibers was studied.

The average diameters of nanofibers fabricated with different loadings of WO_3 are presented in Table 1 which indicates that PVC nanofibers fabricated using the WO_3 nanoparticle filler of 35 wt.% have the smallest diameter. According to Fig. 1, the average diameter of PU/PVC nanofibers were 359, 282, 416, and 398 nm for filler percentages of 0, 10, 20 and 30%, respectively.

The morphology of electrospun nanofibers depends on many parameters. Among them, the molecular weight, electrical solution conductivity, voltage, rotation speed of the collector, distances between collector and capillary, feed rate, temperature, and polymer concentration can affect the diameter of nanofibers. While most of the parameters in producing the nanofibers in this study are more and less the same, the molecular weight and especially electrical conductivity of PVC are significantly higher than the ones of the PAV and PU which can play an effective role in reducing the diameter of the nanofibers in case PVC/WO_3 composite [31].

The possible changes in chemical properties caused by filling the nanofibers with WO_3 nanoparticles were investigated using FT-IR analysis, and the results are shown in Fig. 2. The FT-IR spectrum of pure and filled PVA nanofibers

Table 1. The average diameters of nanofibers fabricated with different loadings of WO_3.

	Average diameter (nm)			
WO_3 filler (wt. %)	0	10	20	30
PU/PVC12%	359	282	416	398
PVA12%	500	347	517	505
WO_3 filler (wt. %)	0	10	20	35
PVC30%	73	80	74	55

(Fig. 2a) shows absorption bands of 3298 cm^{-1} (O-H stretching vibration), 2925 cm^{-1} (symmetric and asymmetric C-H bonds), 2854 cm^{-1} (symmetric and asymmetric C-H bonds), 1732 cm^{-1} (C=O or C-O stretching vibration), 1243 cm^{-1} (C–H wagging vibration), 1092 cm^{-1} (C-OH bond), and 846 cm^{-1} (bending vibration). The absorption bands of PVA filled with WO_3 nanoparticles appear at 3317 cm^{-1} (O-H stretching vibration), 2921 cm^{-1} (symmetric and asymmetric C-H bonds), 2852 cm^{-1} (symmetric and asymmetric C-H bonds), 1734 cm^{-1} (conjugated double C=O bond), 1243 cm^{-1} (C–H wagging vibration), 1094 cm^{-1} (C-OH bond), and 809 and 619 cm^{-1} (W-O-W stretching vibration). Therefore, it is found that the OH group interacts with W molecules, thereby forming the nanofibers composite.

From Fig. 2b, FT-IR spectrum of pure and filled PU/PVC nanofibers shows absorption bands at 3326 cm^{-1} (NH), 2926 cm^{-1} (CH), 2855 cm-1 (CH), 1726 cm^{-1} (C=O), 1703 and 1461 cm^{-1} (C=O), 1223 cm^{-1} (CN), 1073 cm^{-1} (C-O-C), and 610 cm^{-1} (C–Cl stretching vibration), whereas those of PU/PVC/WO_3 nanofibers appear at 3322 cm^{-1} (NH), 2921 cm^{-1} (CH), 1703 and 1461 cm^{-1} (C=O), 1413 cm^{-1} (CH2 deformation), 1221 cm^{-1} (CN), 1074 and 1017 cm^{-1} (C-O-C), and 810 and 610 cm^{-1} (W-O-W stretching vibration). Overall, PVA, PVC, and PU/PVC composited with WO_3 nanoparticles show shifted bands with different intensities.

Fig. 2c shows the comparison between FT-IR spectra of pure and filled PVC nanofibers. The absorption bands of 2958 cm^{-1} (C-H stretching vibration), 2927 cm^{-1} (C-H stretching vibration), 1722 cm^{-1} (C=O), 1428 cm^{-1} (CH2 deformation), 1270 cm^{-1} (C-H−rocking vibration), 1072 cm^{-1} (C-C stretching), 1038 cm^{-1} (C-C stretching), 957 cm^{-1} (trans-CH wagging vibration) and 610 cm^{-1} (C−Cl stretching) are indicated in the pure PVC spectrum. For the PVC/WO_3 nanofibers, the bands appear at 2958 cm^{-1} (C-H stretching vibration), 2927 cm^{-1} (C−H stretching vibration), 1721 cm^{-1} (C=O bond), 1259 cm^{-1} (CH−rocking vibration), 1072 cm^{-1} (C-C stretching vibration), 1038 cm^{-1} (C-C stretching vibration), 952 cm^{-1} (trans-CH wagging vibration), and 808 and 608 cm^{-1} (W-O-W stretching vibration), indicating that the mixed impurities (WO_3 nanoparticles) are complex with the polymer matrix.

According to a study of the mechanical properties of electrospun nanofibers the pure PVA, PU/PVC polymers have the highest modulus of elasticity value 201, 35.45, and MPa. The modulus of elasticity was observed to decrease

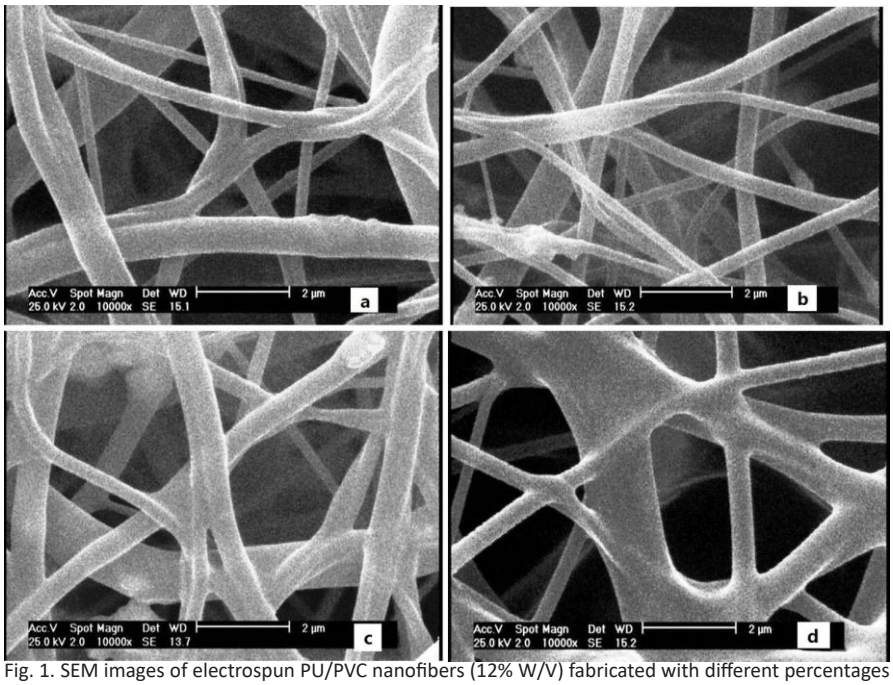

Fig. 1. SEM images of electrospun PU/PVC nanofibers (12% W/V) fabricated with different percentages of WO_3 filler: (a) 0 wt.%, (b) 10 wt. % (c) 20 wt.%, and (d) 30 wt.%.

with adding the filler material to the nanofibers. In the case of PVC the modulus of elasticity value of PU/PVC polymer increases with increasing the filler loading, and is maximized (26.56 MPa) when it is loaded with 30 wt.% WO_3 nanoparticles. The calculated values of tensile strength and the highest elongation at break are found to be 4:74:07 ± 0:329 MPa and 1177:44±571:625 mm for pure

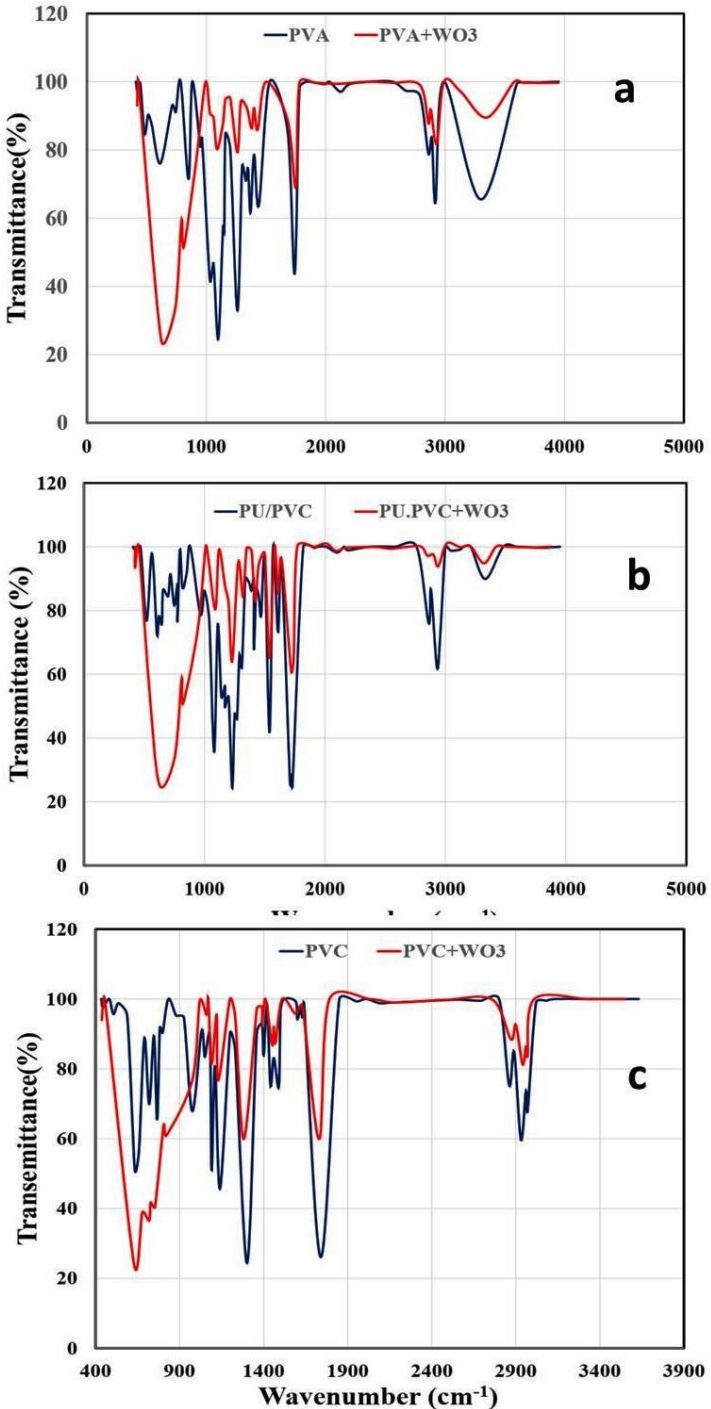

Fig. 2. The comparison between FT-IR spectra of pure and filled PVA(A), PU/PVC(B), and PVC(C) nanofibers.

PVC nanofibers, 0:4±0:025 MPa and 140:53±12:7 mm for PVA nanofibers filled with 20 wt.% WO_3 nanoparticles, and 4:81 ± 1:77 MPa and 678:97 ± 27:21 mm for pure PU/PVC nanofibers.

Effects of filler loading, X-ray tube high voltage, and polymer type on X-ray attenuation

The X-ray shielding properties of some composites were investigated in this study. The intensity of the parallelized X-rays was measured before striking the beam and also after passing through each sample. Then the linear attenuation coefficient was calculated for several accelerator voltages (20.8, 23.7, 26.5, 29.4, 32.2, and 35 kV). The quantity of half-value layer of the manufactured samples has also been calculated to compare their protection capability. Figs. 3, 4, and 5 show HVLs of PVA (12% W/V), PVC (30% W/V), and PU/PVC (12% W/V) nanofibers composites as a function of applied voltages (corresponding to different energies).

In the last three figures, the x-axis shows the amount of accelerating voltage (in kilovolts) and the vertical axis shows the f half-value layer (in cm). The effects of accelerating voltage and also filler concentration can be seen simultaneously

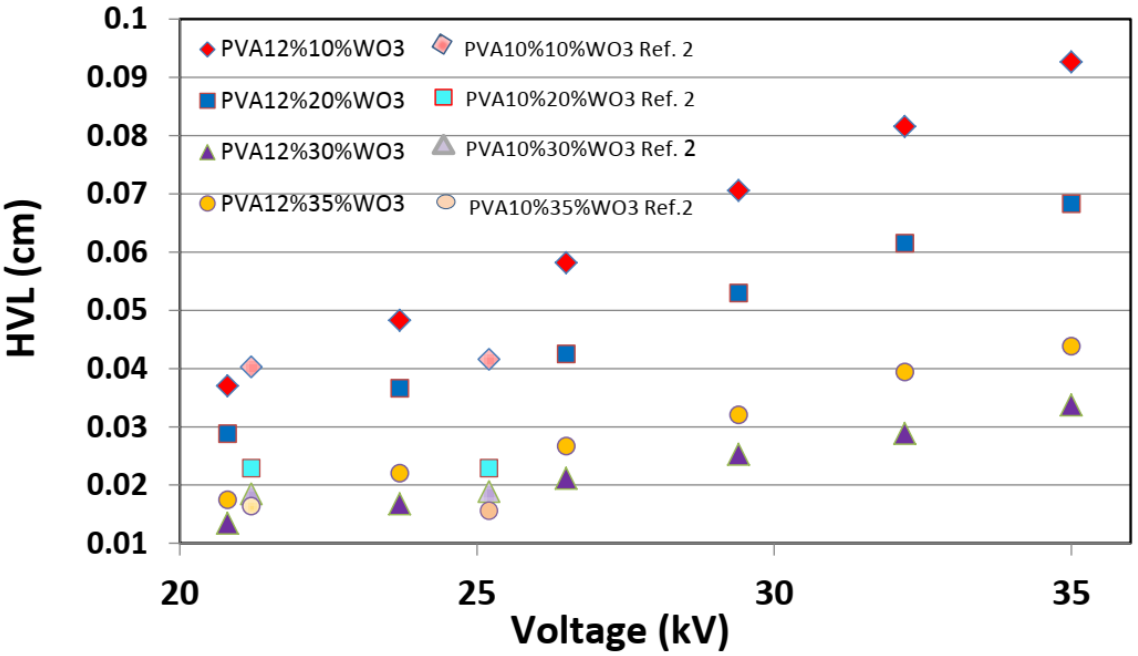

Fig. 3. The half-value layer of PVA electrospun nanofibers with different filler percentage at different voltages in this study and from [2] (20:8 - 35 kV).

Table 2. The half-value layers of PAV/WO_3 obtained in this study and Ref. [2].

	WO_3 concentration (%)	10	20	30	35
	Voltage (kV)	HVL (cm)			
PAV12% Ref. [2]	21.2	0.0403	0.0229	0.0189	0.0156
	25.2	0.0416	0.0299	0.0296	0.0261
PVA15% Ref. [2]	21.2	0.0480	0.0266	0.0240	0.0186
	25.2	0.0781	0.0414	0.0299	0.0298
This study	20.8	0.0370	0.0366	0.0168	0.0220
	23.7	0.0483	0.0425	0.0211	0.0267
	26.5	0.0581	0.0530	0.0253	0.0321

in each figure. Fig. 3 indicates that the HVL of the PVA nanofibers at a fixed voltage decreases with increasing the WO_3 filler loading up to 35 wt. %. Alternatively, HVL is enhanced by increasing the voltage. The lowest HVL is obtained to be 0.0134 cm at the voltage of 20.8 kV using 30 wt. % filler, being about 1.91-fold of that of Pb.

The density and mass attenuation coefficients of PVA/WO_3 nanofibers samples with synthesis parameters almost close to those in our study are

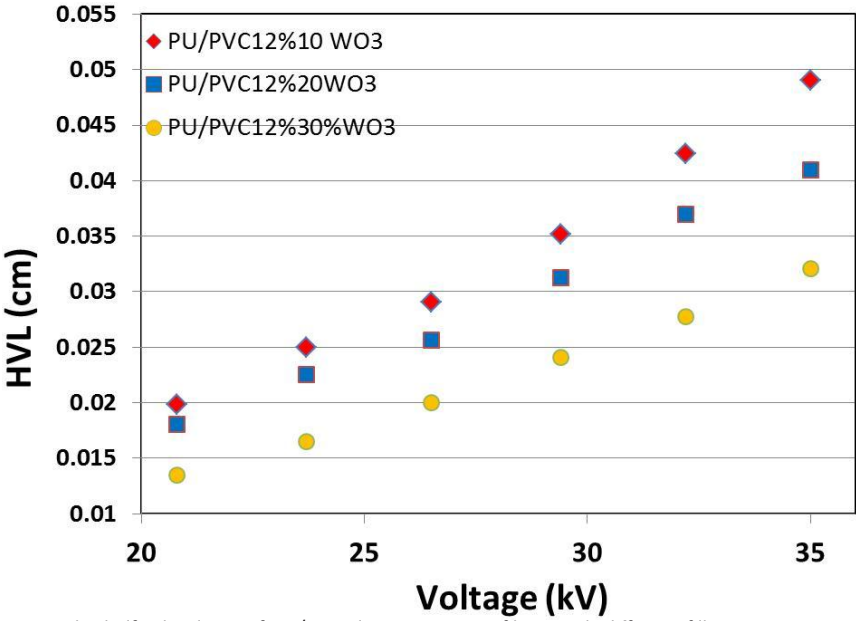

Fig. 4. The half-value layer of PU/PVC electrospun nanofibers with different filler percentage at different voltages (20:8 - 35 kV).

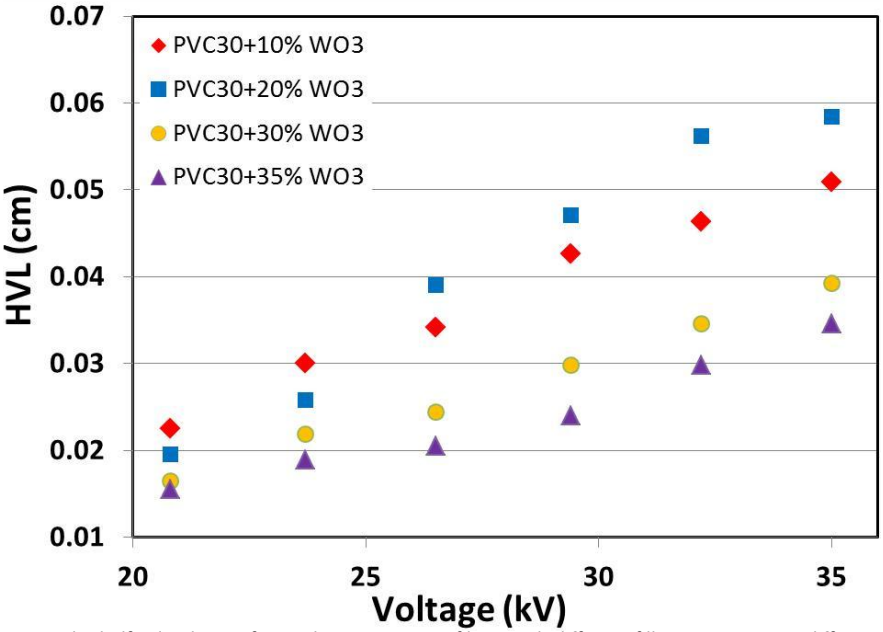

Fig. 5. The half-value layer of PVC electrospun nanofibers with different filler percentage at different voltages (20:8 - 35 kV).

reported by M. Jamil et. al. [2]. The related half-value layers of PVA/WO_3 nanofibers samples were calculated according to the extracted density and mass attenuation coefficients. Table 2 compares the half layers of this study and reference 2 in full. To avoid crowding, only the result of the PVA 12% sample is shown in Fig. 3. The obtained results are in acceptable agreement with each other.

According to Figs. 4 and 5, the lowest HVLs at the voltage of 20.8 kV for PVC and PU/PVC nanofibers are found to be 0.0156 and 0.0135 cm using 35 and 30 wt. % filler loadings, respectively. These HVLs are nearly 2.22- and 1.92 folds of those of Pb at maximum energy of the x-ray spectrum. At high voltage, PU/PVC nanofibers have a lower HVL than that of PVA and PVC nanofibers. In other words, at the voltage of 35 kV, the HVL of PU/PVC nanofibers is 0.032 cm (being 1.32 of HVL of Pb), whereas that of PVA and PVC is 0.0337 cm (1.39 of HVL of Pb) and 0.0346 cm (1.42 of HVL of Pb), respectively. The used half-value layers for Pb at the above comparison were obtained from XCOM simulation at maximum energy of the x-ray spectrum. It should be noted that the composite of PU/PVC with WO_3 has a higher absorption capability of incoming radiation than the other two composites.

CONCLUSION

The electrospinning method was effectively employed to fabricate pure PVA, PVC, and PU/PVC nanofibers, along with PVA, PVC, and PU/PVC nanofibers reinforced with varying concentrations (0 - 35 wt.%) of WO_3 nanoparticles. SEM images and FTIR spectra were used to study the morphological and chemical states of the resulting nanofibers, indicating the effective role of loading percentage in the average diameters and band intensities of the nanofibers. The average diameter of PVA nanofibers was larger than that of PU/PVC nanofibers, reaching a maximum value of 590 nm for a filler loading of 30 wt. %. The smallest diameter was obtained to be 55 nm for PVC nanofibers filed with 35 wt. % WO_3 nanoparticles. By investigating mechanical properties through static tensile tests, the modulus of elasticity of PVC and PU/PVC nanofibers was found to increase with increasing the filler material, achieving maximum values of 35.45 and 26.56 MPa after loading them with 10 and 30 wt. % WO_3 nanoparticles, respectively. The fabricated samples have a linear absorption coefficient comparable to similar values obtained for lead (from XCOM data).

The HVLs of 35 and 30 wt. % WO_3 nanoparticle-fled PVC and PU/PVC nanofibers were 0.01558 and 0.0135 cm, being approximately 2.22- and 1.92-fold compared to those of Pb as evaluated by XCOM calculations at the low voltages. At the high voltages, the HVL of PU/PVC nanofibers was smaller than that of PVA and PVC nanofibers. Therefore, the manufactured samples, especially PU/PVC/WO_3 and PVC/WO_3 nanofibers, have advantages of small half-value layer, significantly lower density than Pb, Lead-free, and flexibility which can pave the way for their use in personal shielding in clinical and nonclinical applications. Due to flexibility, they can easily cover the irradiated organs and therefore, can be good candidates for use as a light, lead-free, and efficient shield for X-rays in diagnostic imaging.

ACKNOWLEDGMENTS

The authors are grateful to the council of the University of Kashan for supporting this work.

CONFLICT OF INTEREST

The authors declare that there is no conflict of interests regarding the publication of this manuscript.

REFERENCES

1. Hyun S-J, Kim K-J, Jahng T-A, Kim H-J. Efficiency of lead aprons in blocking radiation – how protective are they? Heliyon. 2016;2(5):e00117.
2. Jamil M, Hazlan MH, Ramli RM, Noor Azman NZ. Study of electrospun PVA-based concentrations nanofibre filled with Bi_2O_3 or WO_3 as potential x-ray shielding material. Radiat Phys Chem. 2019;156:272-282.
3. Hiorns MP, Saini A, Marsden PJ. A review of current local dose–area product levels for paediatric fluoroscopy in a tertiary referral centre compared with national standards. Why are they so different? The British Journal of Radiology. 2006;79(940):326-330.
4. Hazlan MH, Jamil M, Ramli RM, Noor Azman NZ. X-ray attenuation characterisation of electrospun Bi_2O_3/PVA and WO_3/PVA nanofibre mats as potential X-ray shielding materials. Appl Phys A. 2018;124(7).
5. Oyar O, Kislalioglu A. How protective are the lead aprons we use against ionizing radiation. Diagn Interv Radiol. 2011.
6. Singh KJ, Kaur S, Kaundal RS. Comparative study of gamma ray shielding and some properties of PbO–SiO_2–Al_2O_3 and Bi_2O_3–SiO_2–Al_2O_3 glass systems. Radiat Phys Chem. 2014;96:153-157.
7. Künzel R, Okuno E. Effects of the particle sizes and concentrations on the X-ray absorption by CuO compounds. Applied Radiation and Isotopes. 2012;70(4):781-784.
8. Botelho MZ, Künzel R, Okuno E, Levenhagen RS, Basegio T, Bergmann CP. X-ray transmission through nanostructured

and microstructured CuO materials. Applied Radiation and Isotopes. 2011;69(2):527-530.
9. Tang T, Myers O, Felicelli SD. Computational prediction of effective magnetostriction and moduli of multiphase magnetostrictive composites. International Journal of Engineering Science. 2013;72:1-10.
10. Rahmat AR, Rahman WAWA, Sin LT, Yussuf AA. Approaches to improve compatibility of starch filled polymer system: A review. Materials Science and Engineering: C. 2009;29(8):2370-2377.
11. Jordan J, Jacob KI, Tannenbaum R, Sharaf MA, Jasiuk I. Experimental trends in polymer nanocomposites—a review. Materials Science and Engineering: A. 2005;393(1-2):1-11.
12. Noor Azman NZ, Siddiqui SA, Ionescu M, Low IM. A comparative study of X-ray shielding capability in ion-implanted acrylic and glass. Radiat Phys Chem. 2013;85:102-106.
13. Noor Azman NZ, Siddiqui SA, Ionescu M, Low IM. Synthesis and characterisation of ion-implanted epoxy composites for X-ray shielding. Nuclear Instruments and Methods in Physics Research Section B: Beam Interactions with Materials and Atoms. 2012;287:120-123.
14. Ghaffari-Moghaddam M, Eslahi H. Synthesis, characterization and antibacterial properties of a novel nanocomposite based on polyaniline/polyvinyl alcohol/Ag. Arabian Journal of Chemistry. 2014;7(5):846-855.
15. Cano JM, Marín ML, Sánchez A, Hernandis V. Determination of adipate plasticizers in poly(vinyl chloride) by microwave-assisted extraction. Journal of Chromatography A. 2002;963(1-2):401-409.
16. Lee KH, Kim HY, Ryu YJ, Kim KW, Choi SW. Mechanical behavior of electrospun fiber mats of poly(vinyl chloride)/polyurethane polyblends. J Polym Sci, Part B: Polym Phys. 2003;41(11):1256-1262.
17. Emad Abdoluosefi H, Honarasa G. Fabrication of polyurethane and thermoplastic polyurethane nanofiber by controlling the electrospinning parameters. Materials Research Express. 2017;4(10):105308.
18. Jain P, Pradeep T. Potential of silver nanoparticle-coated polyurethane foam as an antibacterial water filter. Biotechnology and Bioengineering. 2005;90(1):59-63.
19. Gorji M, Jeddi AAA, Gharehaghaji AA. Fabrication and characterization of polyurethane electrospun nanofiber membranes for protective clothing applications. J Appl Polym Sci. 2012;125(5):4135-4141.
20. Choi H-J, Kim SB, Kim SH, Lee M-H. Preparation of electrospun polyurethane filter media and their collection mechanisms for ultrafine particles. Journal of the Air and Waste Management Association. 2013;64(3):322-329.
21. DeMerlis CC, Schoneker DR. Review of the oral toxicity of polyvinyl alcohol (PVA). Food and Chemical Toxicology. 2003;41(3):319-326.
22. Maghrabi HA, Vijayan A, Deb P, Wang L. Bismuth oxide-coated fabrics for X-ray shielding. Textile Research Journal. 2015;86(6):649-658.
23. Haider A, Haider S, Kang I-K. A comprehensive review summarizing the effect of electrospinning parameters and potential applications of nanofibers in biomedical and biotechnology. Arabian Journal of Chemistry. 2018;11(8):1165-1188.
24. Noor Azman NZ, Siddiqui SA, Hart R, Low IM. Effect of particle size, filler loadings and x-ray tube voltage on the transmitted x-ray transmission in tungsten oxide—epoxy composites. Applied Radiation and Isotopes. 2013;71(1):62-67.
25. Singh AK, Singh RK, Sharma B, Tyagi AK. Characterization and biocompatibility studies of lead free X-ray shielding polymer composite for healthcare application. Radiat Phys Chem. 2017;138:9-15.
26. Low IM, Noor Azman NZ. Synthesis and Characterization of Pb, Bi or W Compound Filled Epoxy Composites for Shielding of Diagnostic X-Rays. Polymer Composites and Nanocomposites for X-Rays Shielding: Springer Singapore; 2020. p. 45-55.
27. Low IM, Noor Azman NZ. Effect of Bi2O3 Particle Sizes and Addition of Starch into Bi2O3–PVA Composites for X-Ray Shielding. Polymer Composites and Nanocomposites for X-Rays Shielding: Springer Singapore; 2020. p. 107-121.
28. Tekin HO, Singh VP, Manici T. Effects of micro-sized and nano-sized WO_3 on mass attenauation coefficients of concrete by using MCNPX code. Applied Radiation and Isotopes. 2017;121:122-125.
29. Berger MJ, Hubbell JH. XCOM: Photon cross sections on a personal computer. Office of Scientific and Technical Information (OSTI); 1987 1987/07/01.
30. A. Abu Saleem R, Abdelal N, Alsabbagh A, Al-Jarrah M, Al-Jawarneh F. Radiation Shielding of Fiber Reinforced Polymer Composites Incorporating Lead Nanoparticles—An Empirical Approach. Polymers. 2021;13(21):3699.
31. Al-Abduljabbar A, Farooq I. Electrospun Polymer Nanofibers: Processing, Properties, and Applications. Polymers. 2022;15(1):65.